Effect of Flake Graphite Size on Mechanical Properties and Thermal Conductivity of Aluminum Matrix Composites (Postprint)

Authors: Liu Xiaoyun, Wang Wenguang, Wang Dong, Xiao Bolü, Ni Dingrui, Chen Liqing, Ma Zongyi

Date: 2017-04-10T00:00:00+00:00

Abstract

Powder metallurgy was employed to prepare flake graphite-reinforced aluminum matrix (50vol.%Gf/Al) composites with nominal flake sizes of 150, 300, and 500 m, yielding dense composite billets with densities approaching theoretical values. The flake graphite was tightly bonded with the aluminum alloy matrix, with no defects such as cracks or voids observed at the interface. The xy-direction of the flake graphite was essentially parallel to that of the billet; however, due to the influence of the powder metallurgy process, smaller flake graphite exhibited slight misalignment relative to the billet' s xy-direction, which gradually diminished as the flake size increased. The strength of the composites decreased progressively with increasing flake graphite size. The flexural strength of the 150 m flake graphite composite was 82 MPa, decreasing to 39 MPa when the flake graphite size increased to 500 m. The relatively low strength of flake graphite facilitates crack propagation along the graphite interlayers, a phenomenon that becomes more pronounced with increasing flake size, making graphite delamination readily observable in the fracture surface. The thermal conductivity of the composites in the xy-direction increased with flake graphite size, reaching a maximum of 604 W/m ? K, representing a 63% improvement compared to smaller flake graphite. The interfacial heat transfer coefficients of the 300 and 500 m flake graphite composites were slightly lower than theoretical values, whereas that of the 150 m flake graphite composite was significantly lower than the theoretical value. Besides flake graphite size, factors such as shape, distribution, and internal defects also influence the thermal conductivity of the composites.

Full Text

Abstract

Graphite flake reinforced aluminum matrix composites (Gf/Al) with low density, good machinability, and high thermal conductivity are considered excellent heat sink materials for the electronics industry. While liquid-phase methods such as infiltration can produce composites with high thermal conductivity, they often lead to formation of the Al_4C_3 phase, which degrades corrosion resistance. Powder metallurgy can avoid Al_4C_3 formation. In this work, three sizes of graphite flakes (150, 300, and 500 m) were used to investigate the effect of flake size on the strength and thermal conductivity of Gf/Al alloy composites. The 50% Gf/Al alloy (volume fraction) composites were fabricated by powder metallurgy. All three composites achieved densities close to theoretical values. The graphite flakes bonded well with the Al alloy matrix without cracks or pores. The (001)Gf basal planes of the flakes were almost parallel to the circular plane (xy plane) of the composite ingot. However, for smaller flakes, the (001)Gf basal planes were not perfectly parallel to the xy plane due to processing effects, while larger flakes showed better orientation. Composite strength decreased with increasing flake size: the 150 m flake composite exhibited a bending strength of 82 MPa, which dropped to 39 MPa for the 500 m flake composite. Due to the low interlayer strength of graphite, cracks propagated easily along flake layers, becoming more pronounced with larger flake sizes and resulting in observable flake peeling on fracture surfaces. Thermal conductivity in the xy plane increased with flake size, reaching a maximum of 604 $W/(m \cdot K)$—a 63% improvement compared to smaller flakes. The interfacial thermal conductance (hc) of the 300 and 500 m flake composites was slightly lower than theoretical values, while the 150 m flake composite showed significantly lower hc. Besides flake size, shape, distribution, and internal defects also influenced thermal conductivity.

Keywords: graphite flake, aluminum matrix composite, thermal conductivity, mechanical property

Introduction

With the rapid development of electronic devices, increasing power densities in electronic components make effective heat dissipation critical for performance and stability. Constrained by operating conditions, the electronics and semiconductor industries typically employ passive cooling through heat sink materials that transfer heat via conduction. Thermal management materials must therefore possess high thermal conductivity and a coefficient of thermal expansion matched to the substrate to ensure thermal stability and prevent device failure from insufficient heat removal.

Metal matrix composites, fabricated by designed combination of metallic matrices with reinforcements, integrate the high thermal conductivity, low density, and low thermal expansion of reinforcements with the high strength and

good ductility of metal matrices (e.g., Al and Cu), making them widely used as thermal management materials. Early-generation materials such as Cu/W and Cu/Mo exhibited high density and moderate thermal conductivity around 200 W/(m · K). With increasing demands for lightweight electronics, second-generation materials like SiC/Al and Si/Al emerged, offering similar thermal conductivity but only one-third the density. As electronic device integration and power densities continue rising, third-generation materials with thermal conductivity exceeding 400 W/(m · K) have been developed, including vapor-deposited diamond films, diamond/Al, diamond/Cu, and graphite flake/Al (Gf/Al) composites.

Among reinforcement phases, hexagonal graphite flakes (Gf) are a carbon allotrope with (001)Gf basal planes exhibiting thermal conductivity exceeding 1000 W/(m · K) and density of only 2.2 g/cm^3. Graphite' s softness also imparts good machinability to Gf/Al composites, avoiding the processing difficulties of diamond-reinforced metals. Since thermal conductivity is highest within the (001)Gf basal plane, composites are ideally processed to align flakes in a specific direction for optimal thermal performance, which depends critically on the fabrication method.

Primary fabrication methods for Gf/Al composites include liquid-phase and powder metallurgy techniques. Liquid-phase methods tend to align (001)Gf basal planes parallel to the ingot xy plane. However, the relatively large graphite flakes used make complete Al melt infiltration difficult, resulting in poor densification that reduces both thermal conductivity and mechanical properties. Studies by Prieto et al. and Yang et al. added SiC or Si particles between flakes as spacers to improve density, but these lower-conductivity particles introduced numerous interfaces and increased interfacial thermal resistance, yielding composites with only 526 and 390 W/(m · K) thermal conductivity at 89% and 67% reinforcement volume fractions, respectively. Additionally, high melt temperatures in liquid-phase processing can cause Al_4C_3 formation, which degrades both thermal conductivity and corrosion resistance. While recent work shows that controlling pressure, preheat temperature, and cooling rate during squeeze casting can avoid Al_4C_3 formation, the process requirements are stringent.

Powder metallurgy offers lower processing temperatures that prevent Al_4C_3 formation. Pre-mixing of powders facilitates separation of graphite flakes by aluminum alloy particles, improving densification. However, early studies using pure Al matrices and relatively low hot-pressing temperatures resulted in significant density deficits compared to theoretical values, yielding lower thermal conductivity than liquid-phase processed materials. Notably, most research has focused on graphite content effects, while the critical influence of flake size on thermal conductivity remains unreported.

This work investigates Gf/Al composites with different flake sizes fabricated by powder metallurgy. To reduce hot-pressing temperature requirements, 6061 aluminum alloy was selected as the matrix to achieve dense composites at lower temperatures. The effects of flake size on thermal conductivity, mechanical

properties, and microstructural evolution were studied.

Experimental Procedures

Graphite flakes with nominal sizes of 150, 300, and 500 m were used as reinforcements, with 50 m 6061 aluminum alloy powder (Al-1.0%Mg-0.6%Si-0.2%Cu, mass fraction) as the matrix. Composites containing 50 vol% graphite flakes were fabricated by powder metallurgy. The alloy powder and graphite flakes were mixed with alcohol at a 2:1 volume ratio, stirred for 2 h, dried, and loaded into an 80 mm diameter steel die. Vacuum hot pressing was performed at 620°C for 1 h under 50 MPa pressure and 5$×10^{-2}$ Pa vacuum, producing ingots 80 mm in diameter and 50 mm thick. The ingot height direction was defined as the z-direction, with the diameter plane as the xy plane.

For thermal conductivity measurement in the xy plane, 12.7 mm diameter × 3 mm thick discs were cut from the ingots (with the 3 mm thickness along the ingot diameter direction). Thermal diffusivity was measured using a NETZSCH LFA467 laser flash apparatus. Specific heat capacity was measured using a NETZSCH STA 499 C thermal analyzer with DSC samples of 4 mm diameter × 1 mm thickness. Density was measured by Archimedes' principle (three measurements per sample, error < $±$2%). Thermal conductivity was calculated as the product of thermal diffusivity, specific heat capacity, and density.

Graphite flake characterization was performed using a D/max 2500PC X-ray diffractometer (XRD) at 50 kV and 250 mA. Microstructure was examined using Quanta 600 and Supra 55 scanning electron microscopes (SEM) and a Tecnai F20 transmission electron microscope (TEM). Energy-dispersive spectroscopy (EDS) analyzed second-phase composition. TEM samples were prepared by mechanical grinding followed by ion milling. Bending strength was measured using a SHIMADZU AG-100KNG testing machine on 4 mm × 4 mm × 30 mm specimens, testing the xy-direction strength of the composite ingots. Fracture surfaces were analyzed using a Supra 55 SEM.

Results

[FIGURE:1] shows SEM images of different-sized graphite flakes. The actual flake sizes correspond well to nominal sizes, with minor variations in length and width but uniform distribution within each size range. Some flakes exhibit minor edge damage but have smooth surfaces without obvious defects. Flake thickness ranges from 20–30 m and is uniform within individual flakes. [FIGURE:1]d shows a side view of 500 m flakes, revealing ~20 m thickness. All flake sizes show similar thickness, so only the typical 500 m side view is presented.

[FIGURE:2] presents XRD spectra of the graphite flakes. The hexagonal close-packed (hcp) structure shows only two diffraction peaks corresponding to the (002) and (004) planes, indicating strong preferred orientation. No other diffraction peaks are visible, consistent with literature reports.

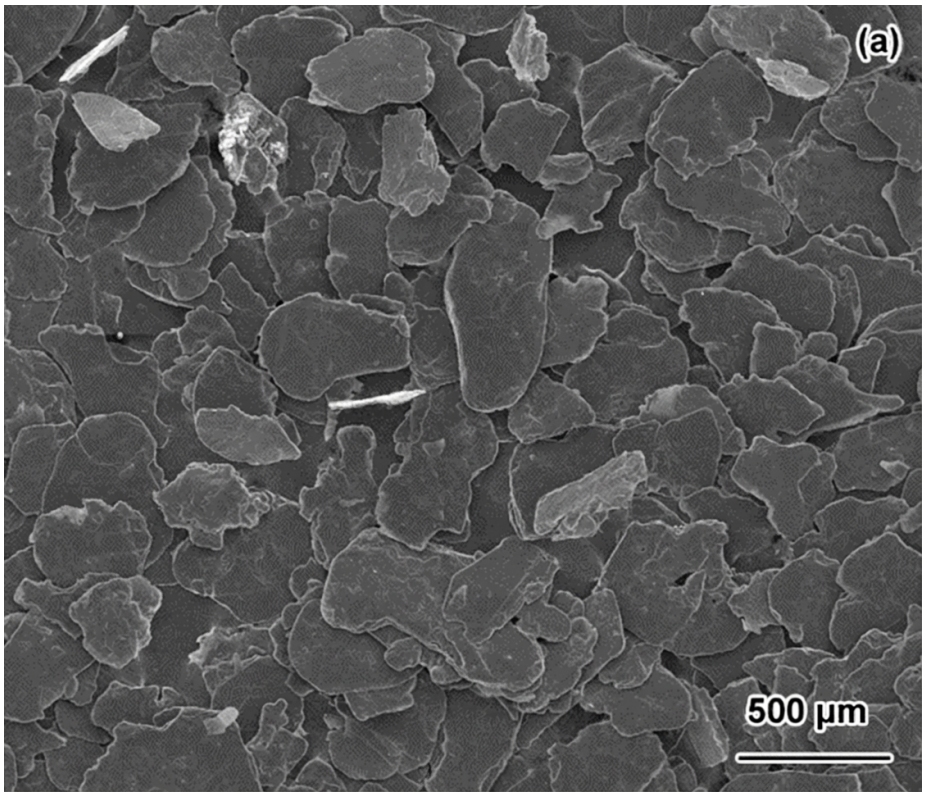

Figure 1: Figure 3

a shows an SEM image of the 150 m Gf/Al composite (z-direction as indicated). Black regions are graphite flakes, gray regions are the Al alloy matrix. Most flakes align horizontally with thicknesses of 20–30 m, similar to [FIGURE:1]d. The low aspect ratio and wet mixing process cause flakes to prefer horizontal distribution during powder loading and drying, resulting in predominantly horizontal alignment after hot pressing. However, some flakes deviate from perfect parallelism with the xy plane due to interactions during mixing and loading, appearing with larger dimensions in the height direction. With increasing flake size, the aspect ratio decreases further, making (001)Gf basal planes more likely to align parallel to the xy plane (

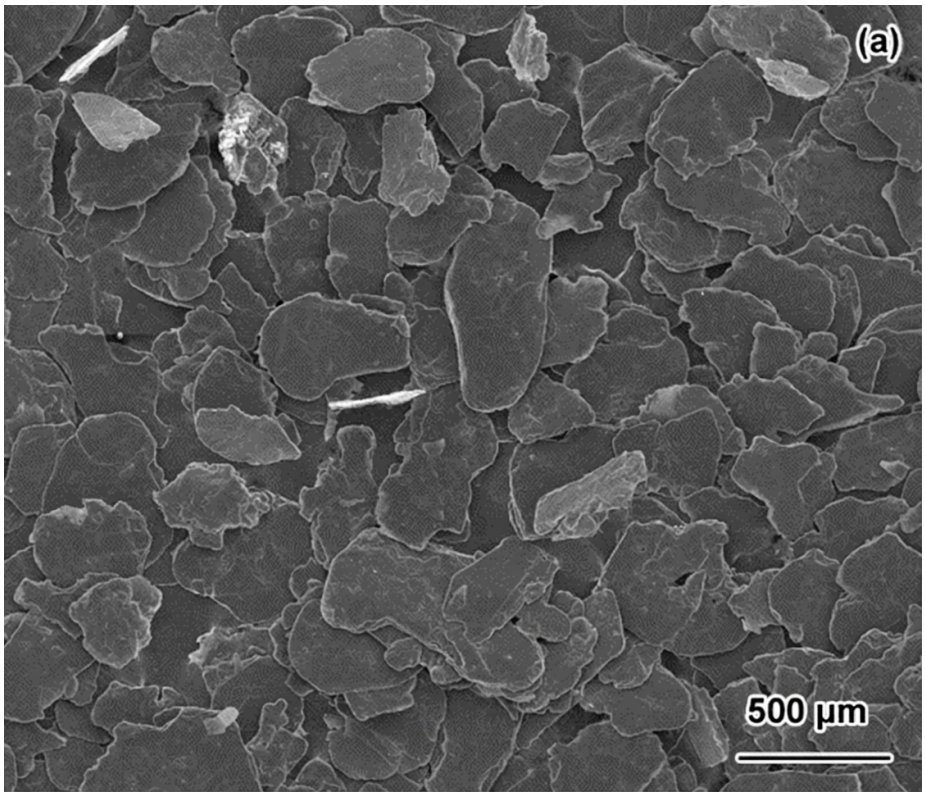

Figure 2: Figure 3

b,c). Flakes remain intact without significant fracture or damage, indicating that wet mixing and vacuum hot pressing do not substantially degrade the flakes, which benefits both thermal conductivity and mechanical properties. Some larger flakes exhibit bending during hot pressing due to surrounding matrix constraints, which appears as increased thickness in the height-direction cross-sections shown in

b,c.

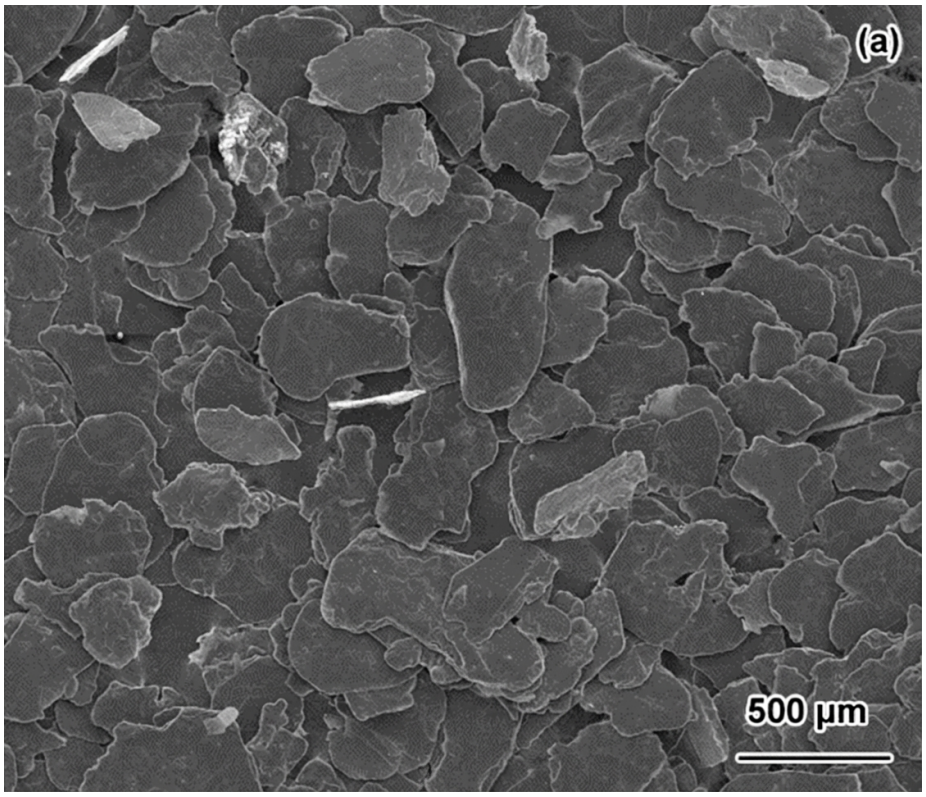

Figure 3: Figure 3

[FIGURE:4]a shows a higher-magnification SEM image of the 150 m composite, revealing white second-phase particles (identified by EDS as Fe-rich phases). Fe is inevitably introduced during alloy powder production, reacting with alloying elements to form Fe-rich phases. Since these form within the alloy powder, their distribution is unaffected by subsequent hot pressing, concentrating them in the matrix independent of flake size ([FIGURE:4]b,c). Gray bands within some flakes (more prominent in larger flakes, [FIGURE:4]b,c) are identified by EDS as aluminum alloy. The 620°C hot-pressing temperature exceeds the 6061 alloy solidus, causing partial melting. Molten Al infiltrates gaps between flake layers or surface defects under pressure, forming alloy bands.

Insets in [FIGURE:4] show magnified flake/matrix interfaces. Similar to literature reports, flakes bond tightly to the matrix without cracks, pores, or Al_4C_3 formation. Fine gray second-phase particles appear discontinuously at interfaces across all flake sizes, identified by EDS as Mg-Si-rich phases. In the annealed 6061 alloy matrix, strengthening Mg_2Si precipitates nucleate and grow preferentially at high-energy flake/matrix interfaces.

TEM analysis of the 500 m composite interface ([FIGURE:5]) confirms tight bonding without cracking or Al_4C_3 formation. The interface is clean with no reaction products. The low hot-pressing temperature and short duration inhibit flake/matrix reactions, consistent with literature reports. [FIGURE:5]b shows an HRTEM image revealing no interfacial compounds and no obvious crystallographic orientation relationship, a common phenomenon in Al matrix composites.

Thermal conductivity values for different composites are listed in . Thermal conductivity increases with flake size: the 150 m composite shows 370 W/(m · K), while the 500 m composite reaches 604 W/(m · K)—a 63% improvement. This exceeds previously reported values for powder metallurgy Gf/Al composites with similar reinforcement content and approaches values for liquid-phase processed materials.

Bending strength values are also shown in . The 150 m composite exhibits 82 MPa strength, which decreases progressively to 39 MPa for the 500 m composite —nearly half the value of the smallest-flake material. Previous Gf/Al research has focused primarily on physical properties with limited mechanical property reporting. Xue et al. prepared 50 vol% Gf/Al composites with 500 m flakes, achieving 35 MPa strength by vacuum hot pressing (similar to this work) but only 28.4 MPa by infiltration processing.

[FIGURE:6] shows fracture surface morphologies of bending specimens. The 150 m composite exhibits layered fracture characteristics ([FIGURE:6]a), indicating good flake alignment parallel to the xy plane. At higher magnification ([FIGURE:6]b), most flakes show fracture rather than delamination, demonstrating that crack propagation occurs within flakes. At 300 m flake size ([FIGURE:6]c,d), flake fracture decreases markedly and extensive flake peeling appears, with smooth flake surfaces visible in the fracture. At 500 m ([FIG-

URE:6]e,f), flake delamination becomes the dominant fracture mechanism.

The composites show good flake/matrix bonding without debonding, and near-theoretical density eliminates porosity defects, contributing to superior strength compared to reported materials. Some alloy infiltration into flake gaps ([FIGURE:4]) also strengthens the material by filling defects. During bending, the higher-strength aluminum alloy constrains the lower-strength graphite, causing cracks to initiate in flakes. Weak interlayer bonding in graphite facilitates crack propagation along flake layers. In small flakes, short crack propagation distances and strong matrix constraint result in flake fracture. In large flakes, longer interlayer crack propagation paths and reduced constraint produce prominent delamination, which becomes more severe with increasing flake size.

Discussion

Thermal conductivity is a critical property of Gf/Al composites. While early researchers proposed simple rule-of-mixtures predictions considering only reinforcement and matrix conductivities, significant discrepancies with measured values were observed. The reinforcement/matrix interface impedes heat transfer, making interfacial bonding crucial for composite thermal performance. Sidhu proposed the interfacial thermal conductance (hc) to evaluate thermal performance, with various models describing composite thermal conductivity. The Maxwell-Garnett type effective medium approximation (MG-EMA) model is considered accurate for composites with ellipsoidal reinforcements.

Although flake shapes vary somewhat, they can be approximated as flat ellipsoids with circular (001)Gf basal planes (radius a_1) and thickness direction (a_3) as the ellipsoid length. The effective thermal conductivity can be expressed as:

$$K^* = K_m \frac{1 + f(\beta_{11} L_{11} + \beta_{33} L_{33})}{1 - f(\beta_{11} L_{11} + \beta_{33} L_{33})}$$

where K* and K_m are composite and matrix thermal conductivities, f is reinforcement volume fraction, L_{11} and L_{33} are shape factors, and β describes interfacial thermal resistance. Assuming flake (001)Gf basal planes are parallel to the ingot xy plane ($\cos^2 = 1$), the equation simplifies to:

$$K^* = K_m \frac{1 + f\beta_{11}}{1 - f\beta_{11}}$$

with

$$\beta_{11} = \frac{K_c - K_m}{K_m + L_{11}(K_c - K_m)}$$

where K_c is flake thermal conductivity. For axisymmetric ellipsoids, shape factors are:

$$L_{11} = L_{22} = \frac{p^2}{2(p^2-1)} - \frac{p}{2(p^2-1)^{3/2}} \cosh^{-1} p$$

with aspect ratio p = a_3/a_1 and $a_1 = a_2$ as the circular basal plane radius.

Interfacial thermal resistance is concentrated at zero-thickness interfaces and described by the Kapitza radius α = a_k/a, where a_k = R_K · K_m with R_K = 1/hc as interfacial thermal resistance and hc as interfacial thermal conductance.

Approximating (001)Gf basal planes as circles gives a_1 values of 75, 150, and 250 m for 150, 300, and 500 m flakes. With flake thickness of 20-30 m, a_3 12.5 m. Using K_c = 1200 W/(m · K) for graphite basal planes and K_m = 180 W/(m · K) for 6061 alloy, calculated hc values are 1.788$\times 10^{\{7\},3.022\times 10}\{7\}, and 3.312\times 10\hat{}\{7\}$ W/(m^2 · K).

The MG-EMA model removes flake size effects, so hc should be consistent across sizes. However, only the 300 and 500 m composites show similar hc, while the 150 m composite exhibits lower hc, indicating additional influencing factors. The model assumes perfect flake alignment parallel to the xy plane, but actual composites show some misalignment (

), particularly for smaller flakes more susceptible to powder and processing effects. Since high thermal conductivity occurs only within the (001)Gf basal plane, misorientation reduces composite thermal conductivity and apparent hc.

Additionally, graphite conducts heat via phonons, while metals have poor phonon thermal conductivity. The interface scatters phonons, creating interfacial thermal resistance. As shown in [FIGURE:4], flake/matrix interfaces contain only minor Mg-Si phases, and TEM results show clean, well-bonded interfaces without reaction products. Therefore, the acoustic mismatch model (AMM) gives:

$$h_c \approx \frac{2\rho_m c_m \nu_m \nu_r}{\rho_m \nu_m + \rho_r \nu_r}$$

where , c, and are density, specific heat, and phonon velocity, with subscripts c, m, and r denoting composite, matrix, and reinforcement. Parameters for the AMM model are listed in (using pure Al data for 6061 alloy where necessary). AMM calculations yield hc = 4.579$\times 10\hat{}\{7\}$ W/(m^2 · K) for 50% Gf/Al composites.

Results show that 300 and 500 m flake composites have hc slightly below theoretical AMM values, while the 150 m composite shows significantly lower hc. Since MG-EMA calculations remove size and content effects, other factors must influence hc. First, unlike some reports, these composites achieve high density near theoretical values (), eliminating porosity effects, particularly at flake/matrix

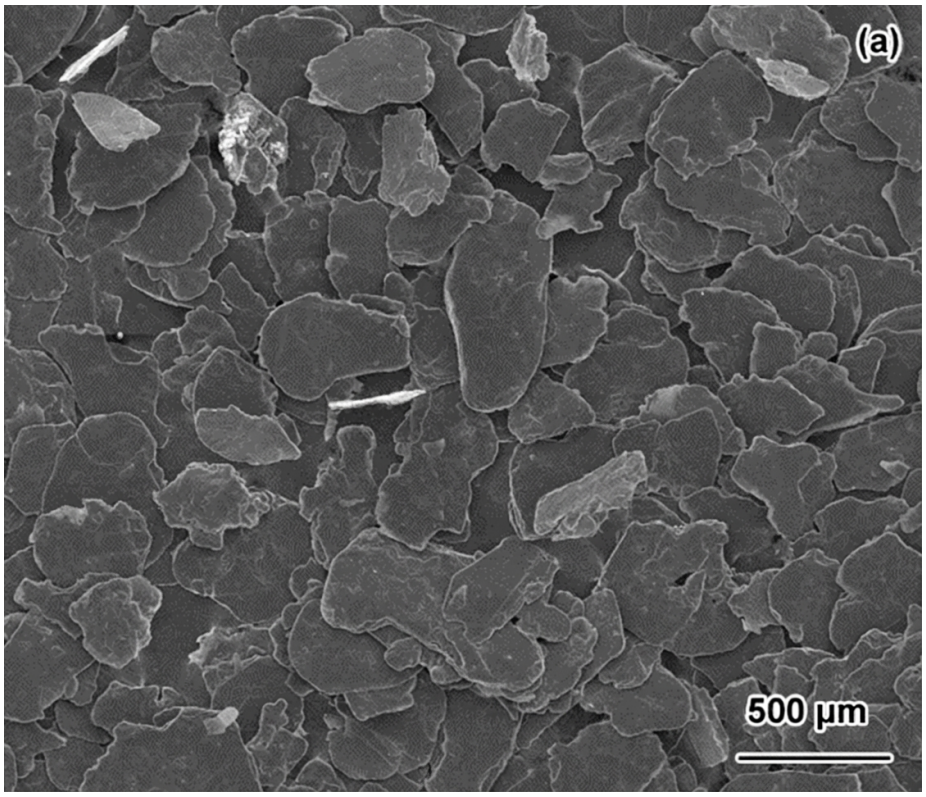

Figure 4: Figure 3

interfaces. Second, actual flakes are not perfectly circular as assumed ([FIGURE:1]), introducing calculation errors. Third, (001)Gf basal planes are not perfectly parallel to the xy plane, especially for smaller flakes whose orientation is more easily disturbed. Finally, internal flake defects allow alloy infiltration ([FIGURE:4]), impeding heat transfer within flakes and affecting hc. Therefore, flake shape, distribution, and internal defects likely cause the MG-EMA calculated hc to be lower than AMM theoretical values, with orientation misalignment being the primary reason for the notably lower hc in the 150 m composite.

Conclusions

(1) Dense 50% Gf/Al composites with different flake sizes were fabricated by powder metallurgy, achieving densities near theoretical values. The (001)Gf basal planes were essentially parallel to the ingot xy plane, with tight flake/matrix bonding and no interfacial cracks or pores.

(2) Composite strength decreased progressively with increasing flake size. The 150 m flake composite exhibited the highest bending strength of 82 MPa, decreasing to 39 MPa for the 500 m flake composite. Larger flakes showed more pronounced flake peeling on fracture surfaces.

(3) Thermal conductivity increased with flake size, reaching 604 W/(m · K) for the 500 m composite—63% higher than the 150 m composite. The interfacial thermal conductance of 300 and 500 m composites was slightly below theoretical values, while the 150 m composite showed significantly lower hc. Besides flake size, shape, distribution, and internal defects substantially influence composite thermal conductivity.

References

[1] Sidhu S S, Kumar S, Batish A. Metal Matrix Composites for Thermal Management: A Review [J]. Crit. Rev. Solid State Mater. Sci., 2016, 41(2): 132

[2] Mathias J D, Geffroy P M, Silvain J F. Architectural optimization for microelectronic packaging [J]. Appl. Therm. Eng., 2009, 29: 2391

[3] Rawal S. Metal-matrix composites for space applications [J]. JOM., 2001, 53(4): 14

[4] Xia Y, Song Y Q, Cui S, et al. Progress in thermal management materials [J]. Mater. Rev., 2008, 22 (01): 4

[5] Xue C, Yu J K. Enhanced thermal transfer and bending strength of SiC/Al composite with controlled interfacial reaction [J]. Mater Des., 2014, 53:74

[6] Liu X Y, Wang W G, Wang D, et al. Effect of nanometer TiC coated diamond on the strength and thermal conductivity of diamond/Al composites [J]. Mater. Chem. Phys., 2016, 182: 256

[7] Yoshida K, Morigami H. Thermal properties of diamond/copper composite material [J]. Microelectron. Reliab., 2004, 44: 303

[8] Fu H, Huang Y, Wu H et al. Synthesis by Vacuum Infiltration, Microstructure, and Thermo-Physical Properties of Graphite-Aluminum Composite [J]. Adv. Eng. Mater., 2016, 18: 1609

[9] Shao XZ, Sum WC, Jin ZX, et al. Modeling the in-plane thermal conductivity of a graphite/polymer composite sheet with a very high content of natural flake graphite [J]. Carbon. 2012, 50: 5052

[10] Li W, Liu Y, Wu G. Preparation of graphite flakes/Al with preferred orientation and high thermal conductivity by squeeze casting [J]. Carbon. 2015, 95: 545

[11] Kurita H, Miyazaki T, Kawasaki A, et al. Interfacial microstructure of graphite flake reinforced aluminum matrix composites fabricated via hot pressing [J]. Composites., 2015, 73A: 125

[12] Prieto R, Molina J M, Narciso J, et al. Thermal conductivity of graphite flakes-SiC particles/metal composites [J]. Composites., 2011, 42A: 1970

[13] Yang Y, Huang Y, Wu H, et al. Interfacial characteristic, thermal conductivity, and modeling of graphite flakes/Si/Al composites fabricated by vacuum gas pressure infiltration [J]. J. Mater. Res., 2016, 31: 1723

[14] Prieto R, Molina J M, Narciso J, et al. Fabrication and properties of graphite flakes/metal composites for thermal management applications [J]. Scr. Mater., 2008, 59: 11

[15] Chen J K, Huang I S. Thermal properties of aluminum-graphite composites by powder metallurgy [J]. Composites., 2013, 44B: 698

[16] Wang D, Xiao B L, Wang Q Z, et al. Friction stir welding of SiCp/2009Al composite plate [J]. Mater. Des., 2013, 47: 243

[17] Huang Y, Ouyang Q B, Guo Q, et al. Graphite film/aluminum laminate composites with ultrahigh thermal conductivity for thermal management applications [J]. Mater. Des., 2016, 90: 508

[18] Zhou C, Huang W, Chen Z, et al. In-plane thermal enhancement behaviors of Al matrix composites with oriented graphite flake alignment [J]. Composites., 2015, 70B: 256

[19] Wang D, Xiao B L, Wang Q Z, et al. Evolution of the Microstructure and Strength in the Nugget Zone of Friction Stir Welded SiCp/Al-Cu-Mg Composite [J]. J. Mater. Sci. Technol., 2014, 30(1): 54

[20] Xue C, Bai H, Tao P F, et al. Thermal conductivity and mechanical properties of flake graphite/Al composite with a SiC nano-layer on graphite surface [J]. Mater. Des., 2016, 108: 250

[21] Nan C W, Birringer R, Clarke D R, et al. Effective thermal conductivity of particulate composites with interfacial thermal resistance [J]. J. Appl. Phys., 1997, 81: 6692

[22] Aerospace structural metals database https://cindasdata.com/Applications/ASMD/?subactionreload%3Amcode&mname=2124&mcode=3221

[23] Molina J M, Louis E. Anisotropy in thermal conductivity of graphite flakes-SiCp/matrix composites: Implications in heat sinking design for thermal management applications [J]. Mater. Charact., 2015, 109: 107

[24] Shenogin S, Gengler J, Roy A, et al. Molecular dynamics studies of thermal boundary resistance at carbon-metal interfaces [J]. Scr. Mater., 2013, 69: 100

[25] Chu K, Jia C, Liang X, et al. Modeling the thermal conductivity of diamond reinforced aluminium matrix composites with inhomogeneous interfacial conductance [J]. Mater. Des., 2009, 30: 4311

[26] Zhou C, Ji G, Chen Z, et al. Fabrication, interface characterization and modeling of oriented graphite flakes/Si/Al composites for thermal management applications [J]. Mater. Des., 2014, 63: 719

Figures

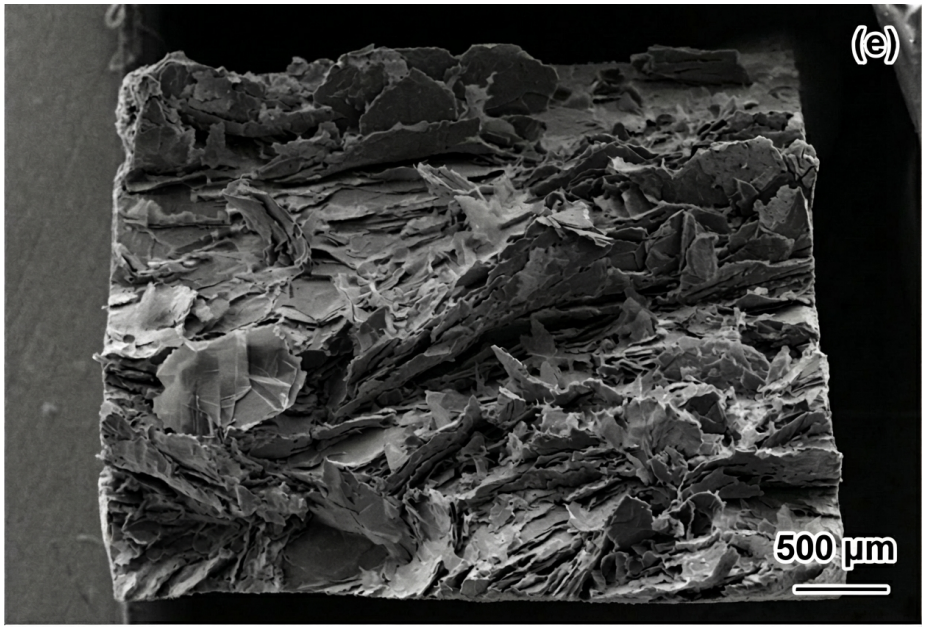

Figure 5: Figure 15

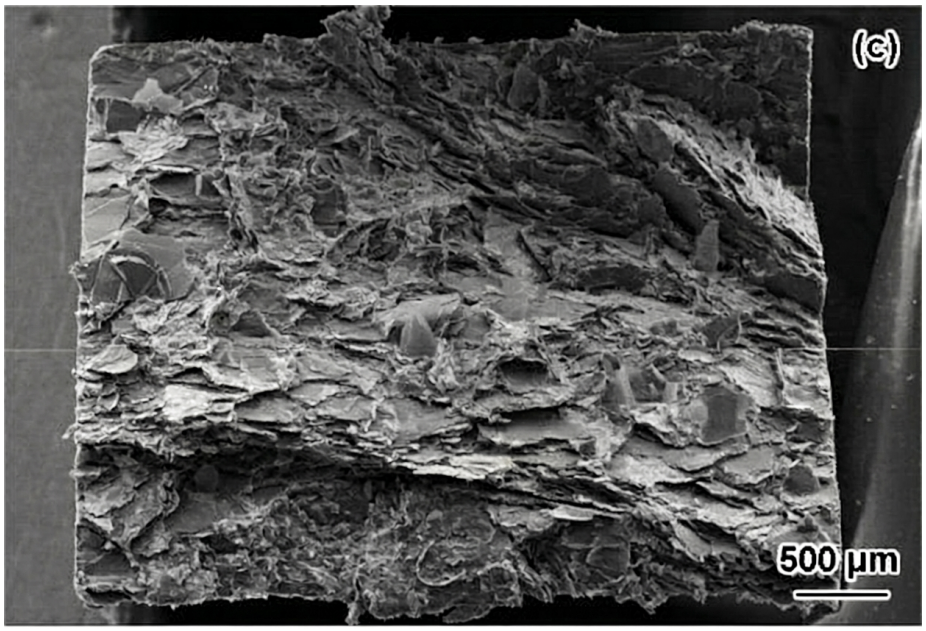

Figure 6: Figure 19